Chinese Chemical Letters 37 (2026) 112028

Contents lists available at ScienceDirect

Chinese Chemical Letters

journal homepage: www.elsevier.com/locate/cclet

Real-time analysis of pyriproxyfen using FA1-targeting albumin-based supramolecular probe with enhanced anti-interference performance

Mingjun Yang, Zhongyong Xu*, Lei Wang, Mingle Li, Xiaoqiang Chen, Bin Liu*, Xiaojun Peng

College of Material Science and Engineering, State Key Laboratory of Fine Chemicals, Shenzhen University, Shenzhen 518060, China

ARTICLE INFO

Article history:
Received 15 July 2025
Revised 23 October 2025
Accepted 27 October 2025
Available online 28 October 2025

Keywords:
Pyriproxyfen
Anti-interference
Albumin
FA1-targeting
Supramolecular probes

ABSTRACT

Given the widespread use of pyriproxyfen (PPF) in public health and agricultural pest management, accurate residue monitoring is critical to ensuring food safety, preserving ecological equilibrium, and protecting human health. While fluorescent sensing techniques represent promising paradigm for PPF detection, existing probes often lack rapid response and high specificity. To address this issue, we present the development of a novel FA1-targeting albumin-based supramolecular probe (DOCD@ALB) for the ratiometric detection of PPF. The strategy design minimizes competitive interference from DS1-binding compounds (*e.g.*, epicatechin), thereby significantly improving its detection accuracy and specificity. When integrated with a smartphone-assisted portable sensing device, the DOCD@ALB system enables on-site PPF quantification in tea matrices, demonstrating its clear translational potential. These findings highlight the pivotal role of binding site selection in modulating the sensing performance of the supramolecular probe system, offering a robust analytical tool with implications for food safety surveillance and environmental protection.

© 2026 Published by Elsevier B.V. on behalf of Chinese Chemical Society and Institute of Materia Medica, Chinese Academy of Medical Sciences.

Pyriproxyfen (PPF), a highly effective insect growth regulator, has been widely utilized in agricultural pest control, public health mosquito management, and veterinary ectoparasite treatment [1–4]. However, increasing concerns have been raised regarding its potential risks to ecological systems and human health due to long half-life (5–48 days) in environment. Studies have shown that PPF is highly toxic to aquatic invertebrates and can disrupt aquatic ecosystems by affecting non-target species' molting and reproduction. Moreover, PPF easily accumulates in animal fat [5], potentially posing a threat to human health. The residue issue of PPF is directly related to food safety and international trade [6]. Various countries have established stringent maximum residue limits (MRLs) for PPF in agricultural products (Table S1 in Supporting information) [7]. For instance, the European Union has set the MRLs for PPF in fruits and vegetables at 0.01–0.5 mg/kg, while China has set the limit for orange, mandarin, and tangerine at 2 mg/kg [8]. Therefore, the detection of PPF in food matrices and environmental is of critical importance.

Conventional analytical methods for PPF detection, including high-performance liquid chromatography (HPLC), liquid chromatography-tandem mass spectrometry (LC-MS/MS), photoelectrochemical sensor, and gas chromatography-mass spectrometry (GC–MS), face significant practical challenges, such as high instrument costs, complex operational workflows, and prolonged analysis times [9–11]. In contrast, fluorescence-based sensing techniques have emerged as compelling alternatives in recent years, offering advantages including easy-to-use, low cost, rapid response, and modular design versatility [12–23]. In our previous work, we developed a host-guest supramolecular fluorescent probe (HOF@ALB, Fig. 1a), incorporating a fluorescent dye HOF as the guest indicator and the albumin (ALB) as the host, for sensitive detection of PPF based on an indicator displacement assay (IDA) [24]. This system operates through competitive binding at drug site 1 (DS1) of albumin, where PPF displaces HOF to induce measurable fluorescence change. However, the DS1 of albumin serves as the primary binding site for numerous exogenous drugs and endogenous biomolecules, creating critical interference issues [25–29]. Specifically, in complex matrices like tea, the epicatechin (EC), abundants in tea leaves, compete with PPF for DS1 site, leading to the false-positive PPF detection results (Fig. 1b) [30]. This limitation underscores the urgent need for fluorescence probes with enhanced anti-interference capabilities to enable accurate PPF quantification in real-world samples.

To overcome this challenge, a straightforward design strategy involves selecting a site-specific indicator capable of

* Corresponding authors.
E-mail addresses: xzy@szu.edu.cn (Z. Xu), bliu@szu.edu.cn (B. Liu).

https://doi.org/10.1016/j.cclet.2025.112028
1001-8417/© 2026 Published by Elsevier B.V. on behalf of Chinese Chemical Society and Institute of Materia Medica, Chinese Academy of Medical Sciences.

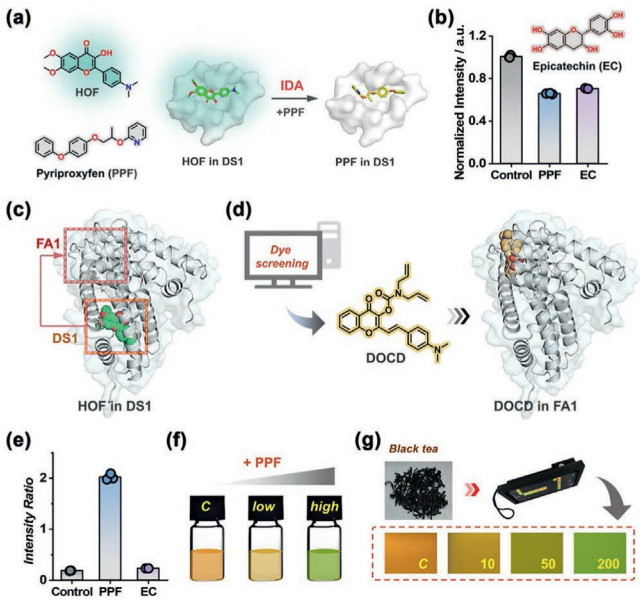


Fig. 1. (a) The chemical structure of HOF and PPF, and the mechanism of HOF@ALB for PPF detection in the previous work. (b) The fluorescent response of HOF@ALB in the presence of PPF and EC. (c) Schematic diagram of the probe design in this work. (d) Chemical structure of screened dye DOCD and its binding complex with albumin. (e) The fluorescent response of DOCD@ALB in the presence of PPF and EC. (f) The diagram of fluorescence color response of DOCD@ALB in the presence of low and high concentration of PPF. (g) Applications of DOCD@ALB in portable devices for PPF in black tea.

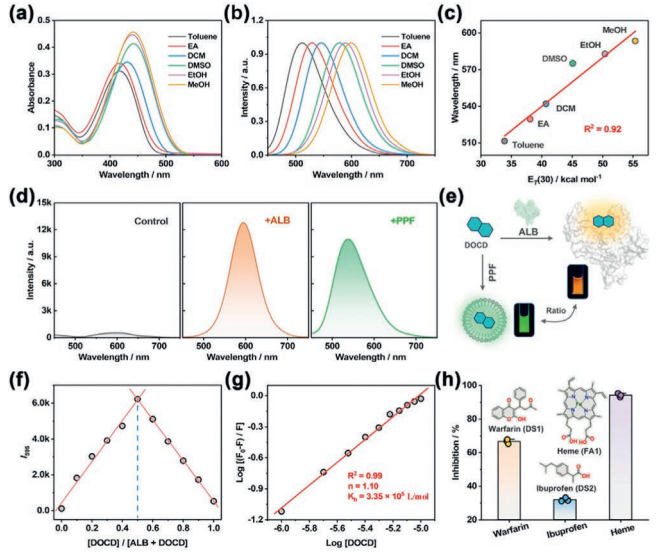


Fig. 2. (a) The absorption spectra and (b) normalized fluorescence spectra of DOCD (10 μmol/L) in six solvents (toluene, ethyl acetate, dichloromethane, DMSO, ethanol, methanol). (c) The dependence of peak wavelength on polarity parameter $E_T(30)$ of each solvent. (d) Fluorescence spectra of DOCD (10 μmol/L), and in the presence of ALB (10 μmol/L) and PPF (200 μmol/L). (e) Schematic diagram of the dual-mode response of DOCD. Inset: photos of solutions emission color under 365 nm UV light. (f) Job's plot analysis by recording the peak intensity in the mixture of DOCD and ALB with different ratios, the overall concentration of mixture remained at 10 μmol/L. (g) Modified Stern-Volmer plot for the quenching ALB by DOCD. (h) Site-specific displacement experiments for DOCD@ALB (10 μmol/L) by adding three drug site indicators (warfarin for DS1, ibuprofen for DS2 and hemin for FA1). $\lambda_{ex} = 430$ nm.

binding to albumin at non-DS1 regions, such as the FA1 site (Fig. 1c) [31,32]. Building on this rationale, we developed 2-(4-(dimethylamino)styryl)-4-oxo-4*H*-chromen-3-yl diallylcarbamate (DOCD), a novel FA1-targeting fluorescent indicator, through a combination of theoretical calculation and experimental validation (Fig. 1d). The molecular docking confirmed that the DOCD docks specifically within the FA1 site of albumin without steric clashes with adjacent residues. When incorporated as a guest indicator into albumin host, the resulting supramolecular probe DOCD@ALB demonstrates exceptional resistance to competitive interference from EC (Fig. 1e). Furthermore, this system possesses a distinct ratiometric fluorescence response to PPF, enabling reliable on-site detection in complex matrices such as tea using portable analytical devices (Figs. 1f and g).

The dye DOCD was easily obtained through our previous work. ^{1}H nuclear magnetic resonance (NMR), ^{13}C NMR and mass spectroscopy were used to characterize of DOCD (Figs. S1–S3 in Supporting information). Immediately, the photophysical properties of DOCD in various solvents were investigated (Table S2 in Supporting information). Fig. 2a shows that the maximum absorbance of DOCD in different solvents located in ranges of 417–461 nm, corresponding to the π-π^* transition [33]. The fluorescent spectra of DOCD exhibited a gradual red-shift as solvent polarities increased (Fig. 2b), demonstrating typical positive solvatofluorochromism [34]. A strong linear correlation ($R^2 = 0.92$) was found between the peak wavelength of DOCD and the $E_T(30)$ values of solvents (Fig. 2c). As shown in Fig. S4 (Supporting information), the fluorescence intensity of DOCD increases with the rise in viscosity, indicating that the probe exhibits viscosity-dependent properties. Next, the fluorescent responses of DOCD to ALB and PPF were examined. DOCD showed minimal fluorescence in an aqueous solution (Fig. 2d). However, in the presence of ALB, it emitted intense orange fluorescence ($\lambda_{em} = 595$ nm), while with PPF, it emitted intense green fluorescence ($\lambda_{em} = 535$ nm). These findings suggest that DOCD can be employed to design a ratiometric fluorescent response probe (Fig. 2e).

To verify the feasibility of the supramolecular probe, the detailed exploration of the binding between DOCD and ALB was conducted. Job's plot unequivocally demonstrates that DOCD and ALB can form a binding complex in a 1:1 molar ratio (Fig. 2f). The binding parameters are calculated using fluorescence data. The calculation of binding constant (K_b) and binding stoichiometry (n) can be conducted by using modified Sterm-Volmer plot [35]. As shown in Fig. 2g and Fig. S5 (Supporting information), the value of K_b was as 3.35×10^5 L/mol, indicating albumin can be considered as a suitable carrier for DOCD. The calculated value of n is 1.1, which is consistent with the Job's plot result. To verify the binding site of DOCD within albumin, the indicator displacement experiments were conducted. Three site-specific inhibitors, including warfarin (for DS1), ibuprofen (for DS2) and hemin (for FA1), were employed to inhibit the fluorescence of DOCD@ALB. Fig. 2h and Fig. S6 (Supporting information) show that >90% inhibition was observed in the presence of hemin, indicating that DOCD preferred binding to the FA1 site of albumin.

The sensing performance of the DOCD@ALB for PPF was firstly evaluated. DOCD@ALB itself shows good photostability. Fig. 3a shows that DOCD@ALB can complete its fluorescent response within 30 s in the presence of PPF, indicating its fast response. As shown in Fig. 3b, the fluorescence intensity at 595 nm of DOCD@ALB exhibited a gradual decline with increasing concentrations of PPF within the lower concentration range spanning from 0 to 10 μmol/L. With further increasing concentration of PPF, the peak at 595 nm continuously decreased, with a gradually increasing new emission peak at 535 nm. Notably, within the lower concentration regime (0–10 μmol/L), a strong linear correlation ($R^2 = 0.98$) was observed between the fluorescence intensity at 595 nm and PPF concentration (Fig. 3c). For higher concentrations (10–100 μmol/L), the intensity ratio (I_{535}/I_{595}) also exhibited excellent linearity with PPF concentration ($R^2 = 0.99$) (Fig. 3d). Based on

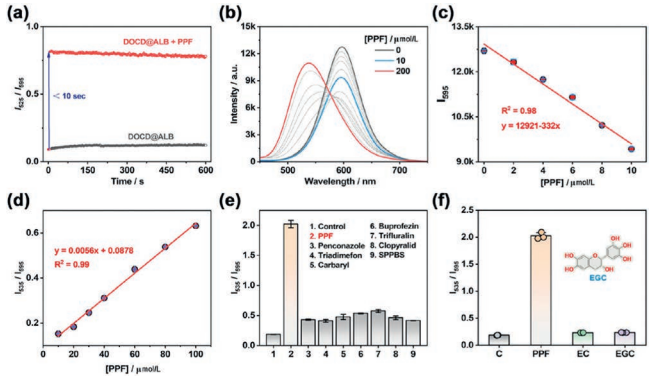


Fig. 3. (a) Time-dependent intensity ratio of DOCD@ALB (10 μmol/L) in the presence and absence of PPF in PBS buffer. (b) Fluorescent spectra of DOCD@ALB with titration of PPF. (c) Relationship between intensity at 595 nm and the concentration of PPF range from 0 to 10 μmol/L. (d) Relationship between intensity ratio (I_{535}/I_{595}) and the concentration of PPF range from 10 μmol/L to 100 μmol/L. (e) The intensity ratio (I_{535}/I_{595}) of DOCD@ALB (10 μmol/L) in the presence of different pesticides (200 μmol/L). (f) The intensity ratio (I_{535}/I_{595}) of DOCD@ALB (10 μmol/L) in the presence of PPF, EC and EGC (200 μmol/L).

the standard deviation method (3σ/slope) [36], the limit of detection was determined to be 0.75 μmol/L (0.25 ppm).

Next, the specificity of DOCD@ALB was studied toward a panel of pesticides (penconazole, triadimefon, carbaryl, buprofezin, triflualine, clopyralid, and SPPBS). As shown in Fig. 3e and Fig. S7 (Supporting information), only PPF induced a comparable ratiomatric fluorescent response. To assess the probe's resistance to interference from DS1-targeting substances, EC and epigallocatechin (EGC), which are commonly found in tea [37], were utilized to test the fluorescent response of DOCD@ALB. As illustrated in Fig. 3f, PPF elicited a robust fluorescence response from the probe, whereas EC and EGC do not elicit significant fluorescence changes. Then, common species, including common ions, amino acids, and surfactants, were also tested. Figs. S7b and c show that none of them can induce a comparable response. These results indicate that the probe exhibits good anti-interference capability (Fig. S8 in Supporting information). In addition, the probe demonstrates good detection stability within the pH range of 6–8 (Fig. S9 in Supporting information). The abovementioned findings indicated that DOCD@ALB is a promising probe for the detection of PPF.

DOCD@ALB exhibited excellent sensing performance for PPF. To further understand the fluorescence response of DOCD@ALB to PPF, the molecular docking was employed. The binding behavior of PPF within the FA1 pocket of albumin was first examined. As shown in Fig. 4a, PPF can bind effectively within the FA1 pocket with a binding energy of −7.80 kcal/mol. Fig. 4b illustrates that at the same binding site, the calculated binding energy for DOCD in FA1 is −7.69 kcal/mol. Through superposition analysis, it is evident that PPF and DOCD overlap almost completely, and both form a hydrogen bond with the amino acid residue TYR160 (Fig. 4c).

Moreover, LigPlot analysis reveals that they share nine identical amino acid residues (LEU115, LEU122, PHE133, LYS136, TYR137, ILE141, TYR160, LIE181, MET184, ARG185, and VAL188) (Fig. 4d), indicating that PPF and DOCD bind at nearly identical positions within the FA1 site. Fig. 4e demonstrates that at high concentrations of PPF, the fluorescence spectrum of the DOCD@ALB is completely consistent with that of DOCD, suggesting that the dye enters the hydrophobic cavity of PPF under high-concentration conditions. Fluorescence lifetime measurements reveal that the fluorescence lifetimes of both DOCD and DOCD@ALB are essentially the same in the present of high concentrations of PPF, indicating that the fluorescence originates from the dyes that have entered the PPF micelles (Figs. 4f and g). Based on the aforementioned results, it can be inferred that the dual-mode

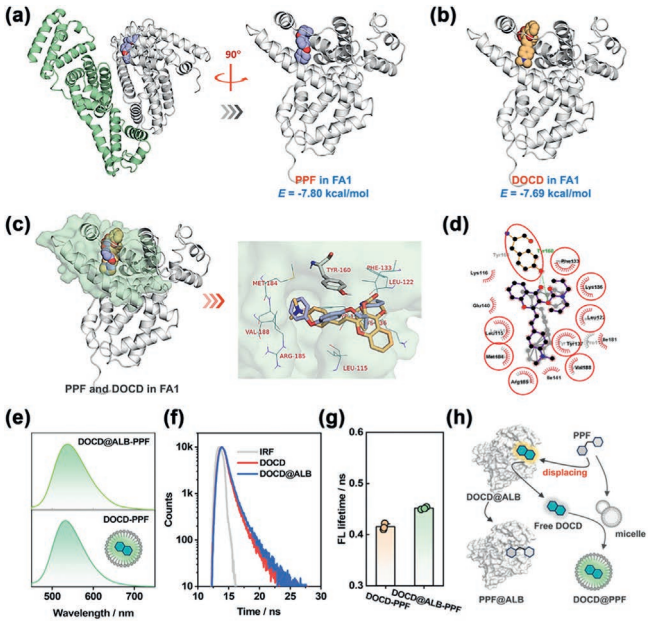


Fig. 4. (a) The calculated binding modes of PPF, (b) DOCD into the FA1 of ALB, and (c) overlap both DOCD and PPF binding into the FA1 of ALB by using the Autodock software. (d) The 2D diagrams of DOCD and PPF jointly binding to the FA1 site of ALB by using the Ligplot. The structure with black bond stands for the DOCD, and that with gray bond stands for the projection planes of PPF. The red circle represents that DOCD and PPF in FA1 binding position share the same amino acid residues. (e) The fluorescence spectra and (f) fluorescence decay curve of DOCD@ALB (10 μmol/L) and DOCD (10 μmol/L) in the presence of PPF (200 μmol/L), $\lambda_{ex} = 430$ nm. (g) The fluorescence lifetime of DOCD and DOCD@ALB in the presence of PPF. (h) Proposed dual-mode fluorescent response mechanism of DOCD@ALB for the detection of PPF.

response mechanism of the probe is as illustrated in Fig. 4h At low concentrations, PPF undergoes an IDA with DOCD, resulting in significant fluorescence quenching. As the concentration of PPF increases, PPF self-assembles into hydrophobic micelles. Upon the entry of free dye molecules into these micelles, a notable ratiometric fluorescence response is observed.

As shown in Fig. 5a, the fluorescence color of the probe undergoes a distinct transition from orange to green with increasing PPF concentration from 0 to 200 μmol/L. Further analysis using chromaticity coordinates reveals that the color of the probe solution changes from (0.54, 0.45) to (0.35, 0.57) (Fig. 5b). These results indicate that the probe can detect PPF through the fluorescence color of the solution [38]. Subsequently, the RGB values of the solutions of DOCD@ALB containing various concentrations of PPF were acquired using RGB recognition software. Upon comparing the green/red (G/R) ratios, as shown in Fig. 5c, it was observed that the fluorescence brightness of the solution with 10 μmol/L PPF was lower than that of the blank solution, indicating fluorescence quenching. As the PPF concentration increased, the G/R value of the solution increases gradually. Moreover, the G/R value demonstrated a good linear relationship ($R^2 = 0.97$) within the concentration range of 0–150 μmol/L (Fig. 5d).

Portable devices, compact, portable, and easy to operate, allow rapid PPF detection, enabling on-site testing anytime, anywhere, and greatly facilitating rapid screening and field decision-making [39–41]. Based on the excellent fluorescence color change of DOCD@ALB for PPF, a mobile phone-assisted portable device developed by our group has been for the portable detection of PPF as our previous work [36,42]. The detection process is illustrated in Fig. 5e. Images captured by the portable device are directly read for RGB values using a mobile phone App. Then, the G/R value of image was obtained easily. Fig. 5f illustrates that the color of the fluorescent images captured by the device changes from orange to

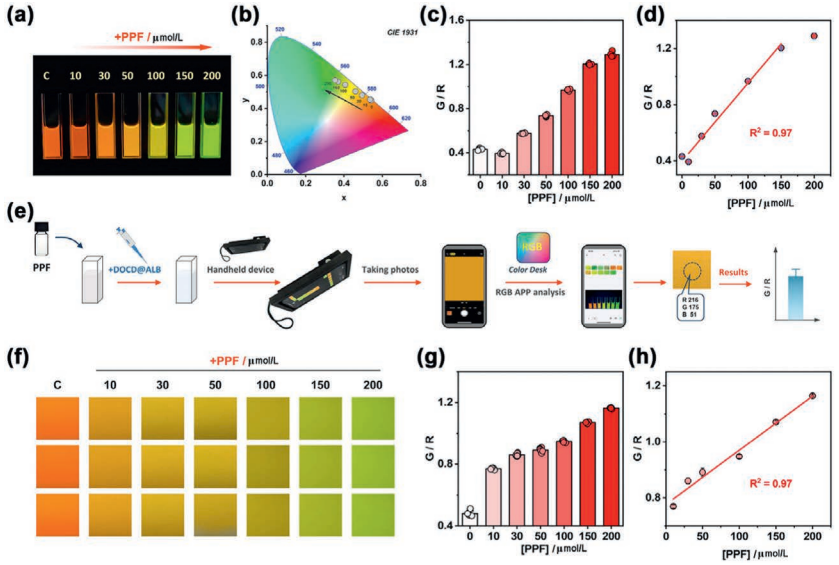


Fig. 5. (a) The photographs of DOCD@ALB in the presence of PPF with various concentrations under 365 nm UV lamp. (b) The fluorescent color change toward PPF on a CIE 1931 graph. (c) The G/R value of DOCD@ALB in the presence of PPF with various concentrations. (d) Relationship between G/R values and the concentration of PPF. (e) Illustration of the application of portable device for PPF analysis based on DOCD@ALB. (f) The photographs and (g) the G/R value of the image of DOCD@ALB from the portable device. (h) Relationship between G/R values and the concentration of PPF. Error bars = ±SD, $n = 3$.

green as the PPF concentration increases. Simultaneously, the G/R values extracted from the images gradually increase as the concentration rises (Fig. 5g). A good linear relationship between the G/R values and the concentration of PPF was observed (Fig. 5h). These results indicate that DOCD@ALB can accomplish portable detection of PPF using a portable device.

To verify the feasibility of DOCD@ALB in actual sample detection, black tea was selected for analysis, because PPF is widely applied for controlling pests in tea gardens [43]. Firstly, the impact of pH on the probe was investigated. The results revealed that the probe exhibited stable detection performance within the pH range of 6.5–9 (Fig. S9 in Supporting information), indicating its applicability for real sample detection. The sensing performance of the probe in detecting black tea extract was first examined. As illustrated in Fig. S10 (Supporting information), a significant fluorescence quenching was observed upon the addition of 10 μmol/L PPF (Fig. S10a). Upon the introduction of 200 μmol/L PPF, the probe demonstrated a pronounced fluorescence ratiometric response. As shown in Figs. S10b and c, fluorescence intensity changes versus PPF concentration at both low and high levels showed a strong linear relationship. The accuracy of the method was evaluated through a spiked recovery experiment. As shown in Table S3 (Supporting information), the method yields recovery rates ranging from 84.95 % to 103.95 %, with RSD values between 0.68 % and 1.07 %, indicating high accuracy. This indicates that the probe can be utilized for analyzing PPF in real sample. Subsequently, tea extracts containing PPF at different concentrations were subjected to portable detection using our portable device. As depicted in Fig. S10d, the portable device was capable of rapidly reading the RGB values of various solutions. The G/R values of the solutions increased with the rising concentration of PPF (Fig. S10e), yet no obvious linear relationship was observed (Fig. S10f). The MRL of PPF in tea, as stipulated by the European Union, is 15 ppm [44]. Fig. S8g demonstrates statistically significant differences in G/R values among the blank sample, samples containing 10 and 200 μmol/L PPF, and the sample with 15 ppm PPF. This finding suggests that the probe, when integrated with the portable detection system, is capable of discriminating between tea samples containing PPF concentrations above the regulatory threshold and those within permissible limits.

In summary, we report the development of a novel supramolecular probe (DOCD@ALB) by strategically localizing the indicator into FA1 site, achieving accurate detection of PPF without the interference from DS1-binding compounds (EC and EGC). The molecular docking confirms that PPF and DOCD compete for overlapping subsites within the FA1 site of albumin, with PPF exhibiting sufficient binding affinity to displace DOCD, thereby inducing a measurable ratiometric fluorescence response. This probe demonstrates exceptional analytical performance, characterized by rapid response (<10 s), sub-ppm detection sensitivity (0.25 ppm), and robust resistance to matrix interferents, crucial for accurate and reliable analysis. Furthermore, the distinct ratiometric color response enables visualization through smartphone-assisted portable device. This work not only introduces a powerful analytical tool for PPF monitoring but also establishes foundational insights for designing albumin-based supramolecular sensors with enhanced selectivity profiles.

CRediT authorship contribution statement

Mingjun Yang: Methodology, Investigation, Data curation, Conceptualization. **Zhongyong Xu:** Writing – original draft, Methodology, Investigation, Data curation. **Lei Wang:** Validation, Resources. **Mingle Li:** Project administration, Data curation. **Xiaoqiang Chen:** Supervision. **Bin Liu:** Writing – review & editing, Supervision, Project administration, Funding acquisition. **Xiaojun Peng:** Supervision, Resources.

Declaration of competing interest

The authors declare that they have no known competing financial interests or personal relationships that could have appeared to influence the work reported in this paper.

Acknowledgments

We thank the financial supports from National Natural Science Foundation of China (No. 22377081), Shenzhen Science and Technology Program (No. JCYJ20230808105411023), Research Team Cultivation Program of ShenZhen University (No. 2023QNT005), and

Liyuan Scholar of Shenzhen University. We also would like to acknowledge the help from Instrumental Analysis Center of Shenzhen University (Xili Campus).

Supplementary materials

Supplementary material associated with this article can be found, in the online version, at doi:10.1016/j.cclet.2025.112028.

References

[1] K. Kupferschmidt, Science 354 (2016) 171–173.
[2] J.J. Sullivan, K.S. Goh, J. Pestic. Sci. 33 (2008) 339–350.
[3] L.E. Guzmán, A.N. Wijetunge, B.F. Riske, et al., J. Am. Chem. Soc. 146 (2024) 8480–8485.
[4] M. Accrombessi, J. Cook, E. Dangbenon, et al., Lancet 401 (2023) 435–446.
[5] H. Liu, X. Yi, J. Bi, et al., J. Hazard. Mater. 365 (2019) 97–106.
[6] J. Feng, Y. Ma, Z. Chen, et al., ACS Sustain. Chem. Eng. 9 (2021) 4988–4999.
[7] H. Abdourahime, M. Anastassiadou, M. Arena, et al., EFSA J. 17 (2019) 5732.
[8] GB2763-2021, National food safety standard—Maximum residue limits for pesticides in food, China, 2021, pp. 496.
[9] G.A. Gómez-Ríos, E. Gionfriddo, J. Poole, et al., Anal. Chem. 89 (2017) 7240–7248.
[10] M. Dong, G. Wen, H. Tang, et al., Food Chem. 269 (2018) 136–141.
[11] J. Fenoll, P. Hellín, C. Marín, et al., J. Agric. Food Chem. 53 (2005) 7661–7666.
[12] X. Li, X. Gao, W. Shi, et al., Chem. Rev. 114 (2014) 590–659.
[13] M.H. Lee, J.S. Kim, J.L. Sessler, Chem. Soc. Rev. 44 (2015) 4185–4191.
[14] Z. Xu, W. Deng, N. Li, et al., Chem. Commun. 60 (2024) 6304–6307.
[15] K. Li, T.B. Ren, S. Huan, et al., J. Am. Chem. Soc. 143 (2021) 21143–21160.
[16] S. Xu, K.C. Yan, Z.H. Xu, et al., Chem. Soc. Rev. 53 (2024) 7590–7631.
[17] Z. Zheng, H. Yu, W.C. Geng, et al., Nat. Commun. 10 (2019) 5762.
[18] Y. Zhao, Y. Mei, J. Sun, et al., J. Am. Chem. Soc. 147 (2025) 5025–5034.
[19] N. Xue, H.Y. Zhou, Y. Han, et al., Nat. Commun. 15 (2024) 1425.
[20] A.C. Sedgwick, J.T. Brewster, T. Wu, et al., Chem. Soc. Rev. 50 (2021) 9–38.
[21] T. Liu, X. Han, X. Sun, et al., Chin. Chem. Lett. 36 (2025) 110170.
[22] F. Zheng, R. Xiao, S. Huang, et al., Chin. Chem. Lett. 36 (2025) 109876.
[23] Z. Xiong, S. Qiu, Y. Wang, et al., Chin. Chem. Lett. 36 (2025) 110002.
[24] Z. Xu, Q. Zheng, N. Li, et al., J. Hazard. Mater. 477 (2024) 135364.
[25] J. Shang, X. Zhang, Z. He, et al., Angew. Chem. Int. Ed. 61 (2022) e202205043.
[26] P. Xing, Y. Niu, R. Mu, et al., Nat. Commun. 11 (2020) 1573.
[27] S. Linciano, G. Moro, A. Zorzi, et al., J. Control. Release 348 (2022) 115–126.
[28] Y. Wang, F. Huo, C. Yin, J. Phys. Chem. B 128 (2024) 1121–1138.
[29] Z. Luo, T. Lv, K. Zhu, et al., Angew. Chem. Int. Ed. 59 (2020) 3131–3136.
[30] M. Zhai, H.L. Wu, S.R. Zhang, et al., Sci. China Chem. 57 (2014) 748–754.
[31] L. Wenskowsky, H. Schreuder, V. Derdau, et al., Angew. Chem. Int. Ed. 57 (2018) 1044–1048.
[32] S. Curry, H. Mandelkow, P. Brick, et al., Nat. Struct. Biol. 5 (1998) 827–835.
[33] Z. Xu, X. Zhao, M. Zhou, et al., Sens. Actuators B: Chem. 345 (2021) 130367.
[34] C. Wang, Q. Qiao, W. Chi, et al., Angew. Chem. Int. Ed. 59 (2020) 10160–10172.
[35] G. Rabbani, E.J. Lee, K. Ahmad, et al., Mol. Pharm. 15 (2018) 1445–1456.
[36] Z. Xu, C. Zeng, Y. Zhao, et al., Food Chem. 410 (2023) 135381.
[37] C. Chen, M. Lin, C. Wahl, et al., J. Am. Chem. Soc. 145 (2023) 7974–7982.
[38] M.S. Woolf, L.M. Dignan, A.T. Scott, et al., Nat. Protoc. 16 (2021) 218–238.
[39] Y. Zhu, J. Wang, H. Xie, et al., Anal. Chem. 94 (2022) 10451–10461.
[40] S. Augustine, A. Venkadesh, S. Kaushal, et al., Anal. Chem. 97 (2025) 9569–9599.
[41] D.C. Christodouleas, B. Kaur, P. Chorti, ACS Cent. Sci. 4 (2018) 1600–1616.
[42] N. Li, Z. Xu, Y. Chen, et al., Sens. Actuators B: Chem. (2024) 135823.
[43] H. Li, Q. Zhong, M. Wang, et al., J. Sci. Food Agr. 102 (2022) 3983–3993.
[44] European Food Safety Authority, EFSA J. 11 (2013) 3489.